

## Differential gene expression by chrysotile in human bronchial epithelial cells

Yoo-Na Seo<sup>a</sup>, Yong-Jin Lee<sup>b</sup> and Mi-Young Lee<sup>a,\*</sup>

<sup>a</sup>Department of Medical Biotechnology, SoonChunHyang University, Asan, Chungnam, Korea; <sup>b</sup>Department of Medicine, SoonChunHyung University, Cheonan, Chungnam, Korea; SoonChunHyung Environmental Health Center for Asbestos Related Disease, Cheonan, Chungnam, Korea

(Received 11 April 2011; received in revised form 16 August 2011; accepted 27 September 2011)

Asbestos exposure has been known to contribute to several lung diseases named asbestosis, malignant mesothelioma and lung cancer, but the disease-related molecular and cellular mechanisms are still largely unknown. To examine the effects of asbestos exposure in human bronchial epithelial cells at gene level, the global gene expression profile was analyzed following chrysotile treatment. The microarray results revealed differential gene expression in response to chrysotile treatment. The genes up- and down-regulated by chrysotile were mainly involved in processes including metabolism, signal transduction, transport, development, transcription, immune response, and other functions. The differential gene expression profiles could provide clues that might be used to understand the pathological mechanisms and therapeutic targets involved in chrysotile-related diseases.

**Keywords:** chrysotile; human bronchial epithelial cells; differential gene expression

### Introduction

Asbestos is a family of six naturally occurring silicate fibers exploited commercially for their desirable physical properties (Frank 1993). They include serpentine class chrysotile, and an amphibole class named amosite, crocidolite, tremolite, anthophyllite and actinolite (Rossana et al. 2009). The inhalation of asbestos fibers has been reported to cause serious lung diseases, including malignant lung cancer, mesothelioma and asbestosis (Park et al. 2008; Loomis et al. 2010). Asbestos was also reported to cause DNA double strand breaks, chromosomal aberrations, and abnormal chromosomal segregations (Nymark et al. 2006, 2007). The molecular mechanism underlying asbestos-associated diseases is thought to be very complex and involves several pathways that need to be clarified.

Chrysotile, also referred to as white asbestos, is the most commonly used asbestos fiber in the building industry worldwide (Dopp et al. 2005). It is a soft, fibrous silicate mineral in the serpentine group of phyllosilicates; as such, it is distinct from other asbestiform minerals in the amphibole group. Its idealized chemical formula is  $Mg_3(Si_2O_5)(OH)_4$ . Chrysotile has been considered to be a human carcinogen by the International Agency for Research on Cancer (IARC), but the disease-related processes at the molecular and cellular level are still unclear.

Recently a variety of pathological and epidemiological research on asbestos-related diseases has been reported; however, the data on the effects of chrysotile on the gene expression profile in cultured lung cells are not available. We examined global gene expression

profiles in human bronchial epithelial cell line BEAS-2B following chrysotile exposure through microarray analysis. The specific analysis for those genes or classes of genes that change their expression during exposure to chrysotile could provide valuable clues in understanding the molecular pathology of asbestos-related disease and in searching for novel therapeutic targets.

### Materials and methods

#### Cell culture and cell viability determination

The human bronchial epithelial cell line BEAS-2B (American Type Culture Collection, Rockville, MD) was maintained in bronchial epithelial cell basal medium (BEBM) supplemented with 2 mL bovine pituitary extract, 0.5 mL insulin, 0.5 mL hydrocortisone, 0.5 mL retinoic acid, 0.5 mL transferrin, 0.5 mL triiodothyronine, 0.5 mL epinephrine, 0.5 mL human epidermal growth factor and 1% penicillin at 37°C in an atmosphere of 5% CO<sub>2</sub> (Al-Wadei and Schuller 2006). Chrysotile asbestos was suspended in BEBM medium, and sonicated and triturated through a 22-gauge needle to obtain a homogeneous suspension, and added directly to culture dish for 48 hr treatment. To determine the cytotoxicity and effects of chrysotile on the cell growth, a trypan blue counting assay was performed.

#### Preparation of fluorescent DNA probe and hybridization

Total RNA was extracted from the cell line using the TRI reagent (MRC, OH) according to the

\*Corresponding author. Email: miyoung@sch.ac.kr

manufacturer's instructions (Riml et al. 2004). Each total RNA sample (30 µg) was labeled with Cyanine (Cy5) conjugated dCTP (Amersham, Piscataway, NJ) by a reverse transcription reaction using reverse transcriptase, SuperScript II (Invitrogen, Carlsbad, California). The labeled cDNA mixture was then concentrated using the ethanol precipitation method. The concentrated Cy5-labeled cDNA was resuspended in 10 µL of hybridization solution (GenoCheck, Korea). Then labeled cDNA was placed on a Roche NimbleGen Human whole genome 12-plex array (Roche NimbleGen, Inc., WI) and covered by a NimbleGen H12 mixer (Roche NimbleGen, Inc., WI). The slides were hybridized for 12 hr at 42°C in a MAUI system (Biomicro systems, Inc., UT). The hybridized slides were washed in 2 × SSC, 0.1% SDS for 2 min, 1 × SSC for 3 min, and then 0.2 × SSC for 2 min at room temperature. The slides were centrifuged at 3000 rpm for 20 s to dry (Kim et al. 2009).

#### *Analysis of microarray expression data*

All the experiments were conducted using three separate array sets for control and the two concentrations of chrysotiles used. Twelve replicates of the Roche NimbleGen Human whole genome were included per chip. An average of three different 60-base oligonucleotides (60-mer probes) represented each gene in the genome. A quality control check was performed for each array, which contained on-chip control oligonucleotides. The arrays were analyzed using an Axon GenePix 4000B scanner with associated software (Molecular Devices Corp., Sunnyvale, CA). Gene expression levels were calculated with NimbeScan Version 2.4 (Roche NimbleGen, Inc., WI). Relative signal intensities for each gene were generated using the Robust Multi-Array Average algorithm. The data were processed based on the median polish normalization method using the NimbeScan Version 2.4 (Roche NimbleGen, Inc., WI). The normalized and log transformed intensity values were then analyzed using GeneSpring GX 7.3.1 (Agilent technologies, CA). Fold-change filters included the requirement that the genes be present in at least 150% of controls for up-regulated genes and less than 67% of controls for down-regulated genes. For each gene, expression fold-changes between groups were derived from the mean expression level in three separate replicates. *P*-values are derived from student *t*-tests using log<sub>2</sub> intensity data assuming equal variance. Differentially expressed genes in each point were selected using a volcano plot method.

#### *Quantitative-real-time RT-PCR*

The mRNA levels for the genes of interest in BEAS-2B following exposure to 20 µg/cm<sup>2</sup> chrysotile were analyzed by quantitative real-time RT-PCR using the ABI Prism 7900 Sequence Detection System (PE Applied Biosystems, www.appliedbiosciences.com). Reaction mixtures contained 10 pmol/µL of each primer and 2 × SYBR Green PCR Master Mix (PE Applied Biosystems, www.appliedbiosciences.com), which includes the HotStarTaq DNA polymerase in an optimized buffer, the dNTP mix (with dUTP additive), the SYBRs Green I fluorescent dye, and ROX dye as a passive reference. Thermal cycling conditions were 50°C for 2 min and 95°C for 10 min followed by 40 cycles of 95°C for 30 s and 60°C for 30 s, 72°C for 30 s. In order to exclude the presence of unspecific products, a melting curve analysis of products was performed routinely after finishing amplification by a high-resolution data collection during an incremental temperature increase from 60°C to 95°C with a ramp rate of 0.21°C/s. We then converted real-time PCR cycle numbers to gene amounts (ng) on the basis of the equation. Primer sequences were as follows (forward and reverse, respectively) GMFB: ACA AGG ATA AAC GCC TGG TG, AAT GAA GCG AGG TTG TCG TT; MAPK9: CCC ATG TCC AGG TCT CAG TT, TGC TCT CCT GCT CTC ACA GA; NFRKB: GGT CTG TCC TGG CTG AGA AG, AGA CCT TGG AAC CCT GGA GT; OSP2: CCT AGG GAG CCT CTT CGA CT, TTT GTG GCA AGA AAG CAC AC; USP18: CCG CTC GAG ACC CAT GAG CA, CGC GGA TCC GCA CTC CAT CT; SMC3: GAG TAG AAG AAC TGG ACA GA, GAT TGT ACC TCA GTT TGC TG.

## **Results**

### *Cytotoxicity by chrysotile in human bronchial epithelial cell*

The viability of BEAS-2B cells was determined by the trypan blue dye exclusion test to determine the number of viable cells present in a cell suspension. It is based on the principle that live cells possess intact cell membranes that exclude trypan blue dye, following exposure to various concentrations of chrysotile for 48 hr (El-Said et al. 2009). Chrysotile exposure reduced cell viability in a concentration-dependent manner as shown in Figure 1. The exposure of BEAS-2B cell to 5, 10 and 20 µg/cm<sup>2</sup> chrysotile resulted in an approximately 20, 45 and 50% decrease in cell viability, respectively. The concentrations of 5 and 20 µg/cm<sup>2</sup> chrysotile, which showed approximately 20% and 50%

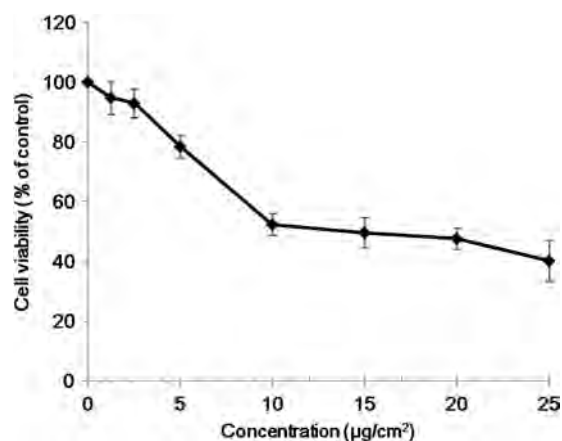


Figure 1. Effect of chrysotile on the viability of human bronchial epithelial cells.

inhibition of cell proliferation, respectively, were used in the subsequent genomic analyses.

### Gene expression profiles

BEAS-2B cells were treated with 5 and 20 µg/cm<sup>2</sup> chrysotile for 48 hr, and total RNA was subjected to microarray analysis. Genes achieving a significant difference ( $P < 0.05$ ) in expression compared to the control in three separate experiments were analyzed. An arbitrary cutoff of 1.5-fold up- or down-regulated was used to further filter the data. In this analysis, 245 genes were up-regulated and 180 genes were down-regulated after 5 µg/cm<sup>2</sup> of chrysotile exposure, and 191 genes were up-regulated and 151 genes were down-regulated after 20 µg/cm<sup>2</sup> chrysotile exposure. A hierarchical clustering was implemented for the visualization and biological interpretation of the gene expression pattern (Figure 2). The cluster image revealed that two groups were well classified with respect to chrysotile exposure.

These up- and down-regulated genes revealed that several genes involved in various functional categories were coordinately induced in the experimental groups when compared with those in the control (Table 1). These genes were involved in processes including metabolism, signal transduction, transport, transcription, development, immune response, cell differentiation, cell cycling, apoptosis and other functions. Genes showing highly altered expression levels were aligned according to the magnitude of the altered expression. The differentially expressed genes that were grouped into functional categories and metabolic pathways based on the KEGG databases are listed in Figure 3, which shows a comparison of the expression levels between the experimental group and the control.

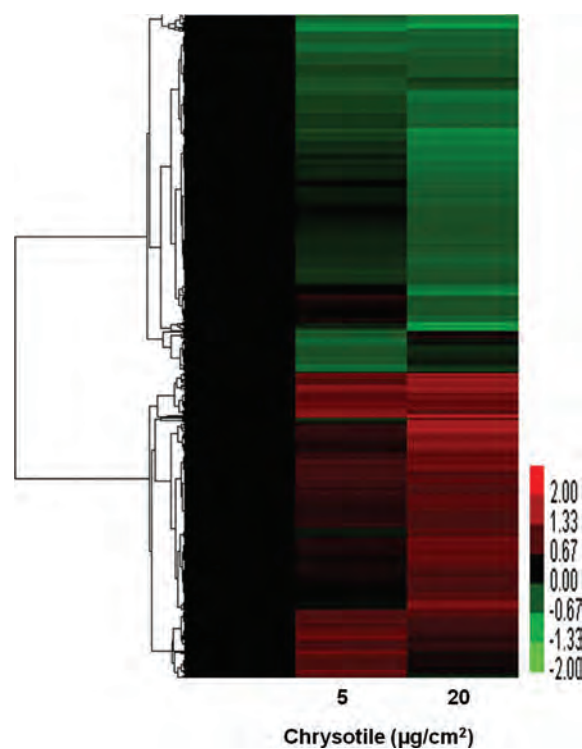


Figure 2. Hierarchical cluster image showing the differential gene expression profiles in human bronchial epithelial cells by 5 and 20 µg/cm<sup>2</sup> of chrysotile treatment. Rows represent genes and columns represent samples. Red and green indicate up-regulation and down-regulation, relative to the control sample, respectively, and black indicates equal expression in control.

### Validation of differentially expressed genes by quantitative real-time PCR

Six differentially expressed genes were selected from the list of differentially expressed genes obtained by microarray analysis. Real-time PCR was conducted for GMFB (glia maturation factor, beta), MAPK9 (mitogen-activated protein kinase 9), NFRKB (nuclear factor related to kappaB binding protein integrin, alpha 1), OSBP2 (oxysterol binding protein 2), USP 18 (ubiquitin specific peptidase 18) and SMC3 (structural maintenance of chromosome 3). The GAPDH gene was used as an endogenous control for all genes. The results from real-time PCR were consistent with those from the DNA microarray (Figure 4).

### Discussion

The central questions in this study concern the classes and magnitude of gene expressions changed in BEAS-2B cells following chrysotile exposure. Genes with expressions altered by at least 1.5-fold up or down with a significance of  $P < 0.05$  were examined. Notable

Table 1. Up- and down-regulated genes based on comparison of gene expression between chrysofile- treated and non- treated human bronchial epithelial cells.

Description	Gene symbol	Fold change			
		5µg/ cm <sup>2</sup>	p- value	20µg/ cm <sup>2</sup>	p- value
<b>&lt; Metabolism &gt;</b>					
Ubiquitin specific peptidase 18	USP18	2.16	0.039	3.25	0.028
Inositol polyphosphate-4-phosphatase, type I, 107kDa	INPP4A	1.49	0.026	2.48	0.049
T-complex 1	TCP1	1.53	0.039	2.47	0.041
Prostaglandin E synthase	PTGES	0.85	0.049	2.44	0.033
Zinc finger homeodomain 4	ZFH4	1.46	0.016	2.29	0.032
Lactate dehydrogenase A	LDHA	2.32	0.0007	1.93	0.005
Oxidative-stress responsive 1	OXS1	1.94	0.020	1.55	0.049
Hydroxyacyl-CoA dehydrogenase	HADH	1.40	0.049	1.22	0.043
H1 histone family, member X	H1FX	0.56	0.008	0.57	0.007
Tetraspanin 4	TSPAN4	0.49	0.025	0.43	0.043
Mastermind-like 1 (Drosophila)	MAML1	0.52	0.038	0.36	0.032
<b>&lt; Signal transduction &gt;</b>					
Glia maturation factor, beta	GMFB	3.02	0.003	2.74	0.049
G protein-coupled receptor 18	GPR18	1.30	0.029	2.73	0.025
START domain containing 8	STARD8	0.91	0.037	2.58	0.011
Serum/glucocorticoid regulated kinase 2	SGK2	1.87	0.016	1.82	0.023
Olfactory receptor, family 3, subfamily A, member 4	OR3A4	2.03	0.048	1.78	0.049
Mitogen-activated protein kinase kinase kinase 7 interacting protein 1	MAP3Kip1	1.89	0.025	2.68	0.014
G protein-coupled receptor 135	GPR135	0.51	0.011	0.78	0.019
Olfactory receptor, family 5, subfamily B, member 17	OR5B17	0.61	0.022	0.41	0.027
<b>&lt; Transport &gt;</b>					
Oxysterol binding protein 2	OSBP2	1.35	0.044	3.21	0.049
Solute carrier family 39 (metal ion transporter), member 11	Slc39a11	1.30	0.049	2.75	0.032
Tubulin, alpha 1b	TUBA1B	1.67	0.018	2.25	0.017
Solute carrier family 25, member 35	SLC25A35	1.14	0.012	2.25	0.032
Cell division cycle 37 homolog (S. cerevisiae)	CDC37	1.94	0.003	2.20	0.019
SNAP-associated protein	SNAPIN	2.05	0.043	2.07	0.049
RAB36, member RAS oncogene family	RAB36	1.30	0.049	1.57	0.049
POM121 membrane glycoprotein (rat)	POM121	0.94	0.019	0.62	0.029
Collagen and calcium binding EGF domains 1	CCBE1	0.47	0.004	0.49	0.045
<b>&lt; Development &gt;</b>					
Small proline-rich protein 3	Spr3	1.38	0.031	2.41	0.039
Mesenchyme homeobox 1	MEOX1	0.54	0.021	0.64	0.012
Transqilin	TAGLN	0.57	0.005	0.62	0.012
5-azacytidine induced 1	AZI1	0.48	0.022	0.042	0.025
<b>&lt; Transcription &gt;</b>					
Structural maintenance of chromosomes 3	SMC3	2.18	0.049	3.02	0.033
Hypothetical LOC389300		2.43	0.016	2.74	0.021
Zinc finger and BTB domain containing 41 homolog	ZBTB41	1.15	0.028	2.51	0.012
Ubiquitin-conjugating enzyme E2N (UBC13 homolog, yeast)	UBE2N	1.52	0.049	2.23	0.042
Forkhead box D4	FOXD4	2.15	0.029	1.67	0.030
PC4 and SFRS1 interacting protein 1	PSIP1	0.44	0.026	0.98	0.049
Actin-binding Rho activating protein	ABRA	0.53	0.014	0.49	0.015
<b>&lt; Immune response &gt;</b>					
UL16 binding protein 3	ULBP3	2.01	0.049	2.26	0.032
Twinfilin, actin-binding protein, homolog 2 (Drosophila)	TWF2	1.89	0.040	2.13	0.029
Aquaporin 9	AQP9	0.48	0.049	0.42	0.026

Table 1 (Continued)

Description	Gene symbol	Fold change			
		5µg/ cm <sup>2</sup>	p- value	20µg/ cm <sup>2</sup>	p- value
<b>&lt; Cell cycle &gt;</b>					
Cell division cycle 37 homolog (S. cerevisiae)	CDC37	1.94	0.003	2.20	0.019
Tumor protein D52-like 1	TPD52L1	0.90	0.042	0.67	0.049
Baculoviral IAP repeat-containing 5 (survivin)	BIRC5	1.20	0.004	0.61	0.049
Anaphase promoting complex subunit 1	ANAPC1	0.76	0.032	0.38	0.014
<b>&lt; Apoptosis &gt;</b>					
Beclin 1 (coiled-coil, myosin-like BCL2 interacting protein)	BECN1	1.95	0.031	2.01	0.044
CD38 molecule	CD38	1.91	0.02	1.95	0.019
Mitogen-activated protein kinase 9	MAPK9	1.72	0.040	1.93	0.049
Tumor necrosis factor receptor superfamily, member 14 (herpesvirus entry mediator)	TNFRSF14	1.69	0.003	1.33	0.040
Signal transducer and activator of transcription 1.91 kDa	STAT1	0.69	0.021	0.83	0.039
Programmed cell death 10	PDCD10	0.45	0.008	0.56	0.049
Notch homolog 2 (Drosophila)	Notch2	0.79	0.038	0.53	0.049
<b>&lt; Inflammatory response &gt;</b>					
Nuclear factor related to kappaB binding protein	NFRKB	1.21	0.049	2.70	0.027
Integrin, alpha 1	ITGA1	1.95	0.039	1.06	0.037
Olfactory receptor, family 7, subfamily A, member 17	OR7A17	0.73	0.049	0.61	0.012
Phosphomannomutase 2	PMM2	0.40	0.049	0.37	0.041
<b>&lt; Cell proliferated &gt;</b>					
Epithelial membrane protein 2	EMP2	1.89	0.029	2.35	0.033
Thy-1 cell surface antigen	THY1	1.27	0.014	1.44	0.023
GLI-Kruppel family member GLI2	GLI2	0.74	0.049	0.42	0.043

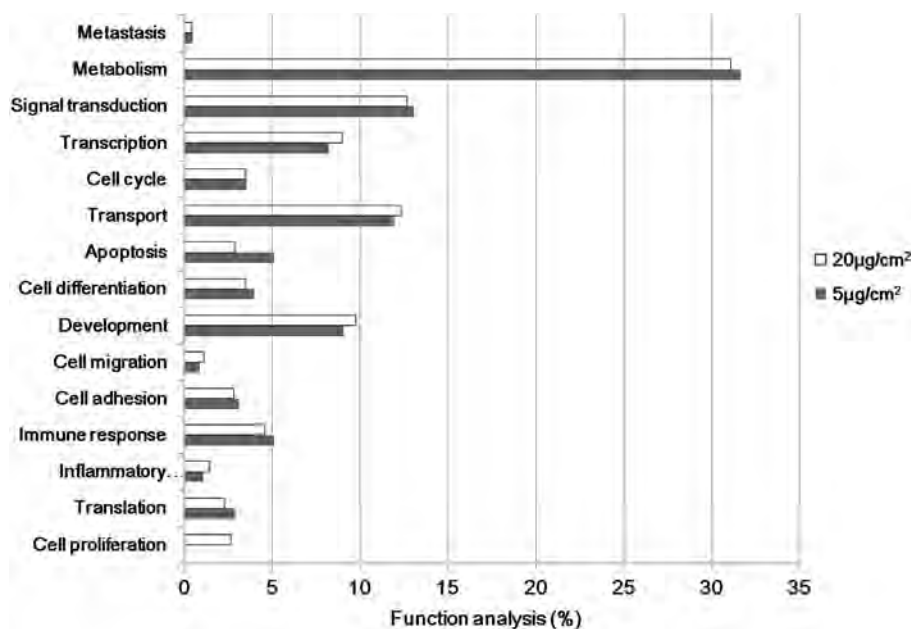


Figure 3. Gene ontology classification of genes based on comparison of gene expression between chrysothile-treated and untreated human bronchial epithelial cells.

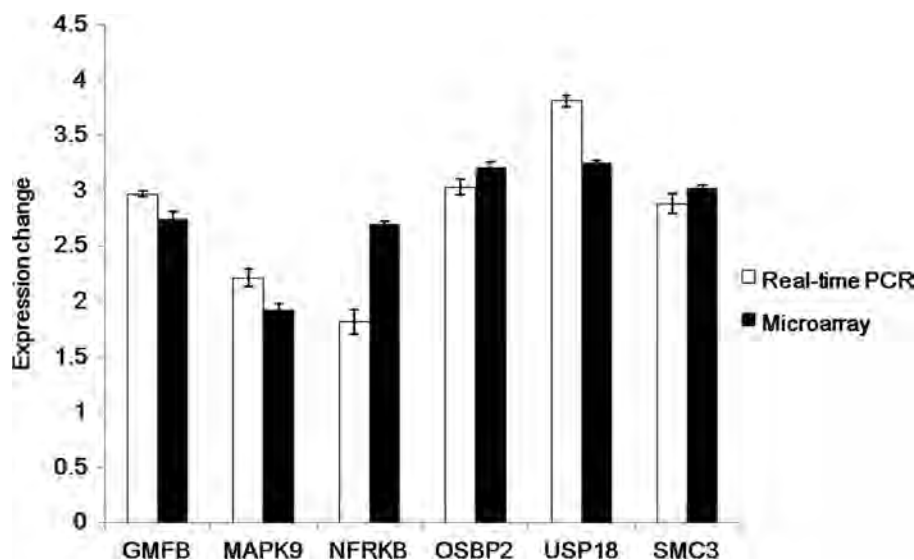


Figure 4. Validation of the differential expression of genes on exposure to chrysotile by quantitative real-time PCR. The mRNA levels were compared between microarray analysis and real-time PCR.

genes in this list were related to processes including metabolism, signal transduction, transport, transcription, development, immune response, cell differentiation, cell cycling, apoptosis and other functions.

Among these genes, a variety of genes involved in sensory perception of smell such as olfactory receptors were found. At 5 ( $IC_{20}$ ) and 20  $\mu\text{g}/\text{cm}^2$  chrysotile ( $IC_{50}$ ), OR3A4 was up-regulated, while OR7A17 and OR5B17 were down-regulated.

Olfactory receptors (ORs) are known to constitute the first element in a biochemical cascade leading to the perception and recognition of smells (Fung et al. 1997; Xu et al. 1999). The initial event in odor perception is the detection of smells by olfactory receptors, which are located on olfactory sensory neurons in the olfactory epithelium of the nose. ORs are seven transmembrane domain G-protein-coupled receptors, which are encoded by a large multigene family. OR genes constitute the largest mammalian gene family, with several hundred genes in the human genome and up to 1550 in the rat genome (Rimbault et al. 2009; Robin et al. 2009). They are expressed not only in the sensory neurons of the olfactory epithelium, but also in various other tissues where their potential functions are largely unknown. It is supposed that the inhalation of chrysotile might affect the olfactory sensory neurons in the olfactory epithelium of the nose, as a variety of OR-related genes were differentially expressed by chrysotile.

The MAPK (mitogen-activated protein kinase) pathway-related genes, named MAPK9 and MAP3-K7IP1, were up-regulated 1.93- and 2.68-fold at 20  $\mu\text{g}/\text{cm}^2$  chrysotile, respectively. The MAPK cascade is composed of sequential series of phosphorylation

(Robin et al. 2009), which include three pathways; extracellular signal-related kinases (ERKs), p38 kinase and c-Jun N-terminal kinases (JNKs) or stress-activated protein kinases (SAPK). ERK2, also known as MAPK1, consists of 44- and 42-kDa Ser/Thr kinases, and is a part of the Ras-Raf-ERK signal transduction cascade often found downstream of growth factor receptor activation (Levchenko et al. 2000). ERK is known to be involved in various cellular proliferation, differentiation and cell cycle processes in response to a variety of extracellular signals. Asbestos fiber has been reported to selectively induce ERK phosphorylation and ERK activity in mesothelial cells, leading to apoptosis and cell proliferation (Shukla et al. 2003). The initiation of the ERK cascade in mesothelial cells by asbestos was due to autophosphorylation of the EGF receptor. Notably, the magnitude of EGF receptor expression depended on the class of the asbestos used. Actually the EGF receptor was enhanced by crocidolite and erionite, whereas it was not by chrysotile (Faux et al. 2000). Moreover, the induction of AP-1 activity by asbestos was thought to be mediated through the activation of MAPK family, ERK1 and ERK2. The activation of ERK by proinflammatory stimuli was also thought to play important roles in innate immune responses and autoimmunity (Ng and Bogoyevitch 2000; Shaul and Seger 2007).

c-Jun N-terminal kinases (JNKs) (also called MAPK9, SAPK, stress activated protein kinase alpha II, stress-activated protein kinase JNK2) are enzymes exhibiting JUN kinase activity, mitogen-activated protein kinase binding, caspase activator activity and other functions (Fusello et al. 2006). MAPK9 is known to be involved in positive regulation of cell morphogenesis,

differentiation, regulation of the JNK cascade, positive regulation of apoptosis and other processes. Up-regulation of the MAPK pathway by chrysotile here might produce the same result as growth factor stimulation by receptor tyrosine kinases, which were coupled to the activation of Ras G-proteins and malignant transformation, as reported earlier (Shapiro 2002). Drugs that selectively down-regulate MAP kinase cascades were proven to be valuable as therapeutic agents to treat malignant diseases (Kortjenann and Shaw 1995).

Glia maturation factor beta (GMFB) is involved in nervous system development, angiogenesis and immune functions. The structures of mouse glia maturation factors beta and gamma reveal homologies with ADF-H (actin depolymerization factor homology) domains and suggest a new function of this protein family. GMFB was suggested to be involved in an inhibition process of IFN beta-1a on activation and apoptosis of LX-2 cells in liver, and as an independent prognostic predictor for ovarian cancer (Li et al. 2010). GMFB was approximately 3-fold up-regulated by chrysotile-exposed bronchial epithelial cells, and the over-expression was confirmed by both microarray and real-time PCR.

Asbestos-induced inflammation and proliferation are thought to be associated with the development of asbestos-associated diseases, asbestos-induced redox change, phosphorylation events and in vitro activated nuclear factor-kappa B (NFkB). Those genes involved in NFkB/IkB pathways, including ubiquitin specific peptidase (USP18), tumor necrosis factor receptor superfamily 14 (TNFRSF14) and inhibitor of kappa light polypeptide gene enhancer in B-cells, kinase beta (IKKB), were detected. Nuclear factors related to kappa B binding protein (NFKB) were 2.70-times up-regulated at 20  $\mu\text{g}/\text{cm}^2$  chrysotile.

Notably, ubiquitin-specific peptidase 18 (USP18) was enhanced approximately 3.25-fold at 20  $\mu\text{g}/\text{cm}^2$  chrysotile. Mutation in ubiquitin-specific peptidase 18 (USP 18) caused hyperactivation of IFN- $\beta$  signaling and suppressed STAT4-induced IFN- production, resulting in enhanced susceptibility to bacterial infection (Malakhova et al. 2003). *N*-Ethyl-*N*-nitrosourea-induced missense mutation in the USP18 gene resulted in an increased inflammatory response (IL-6, type 1 IFN) to salmonella and LPS challenge while paradoxically reducing IFN production during bacterial infection. Thus, USP18 up-regulated by chrysotile might be related to inflammation and cytokine-induced death through reduced IFN-levels.

Previously identified mesothelioma-associated genes, human homologs of asbestos-associated murine genes and other asbestos-related genes already present in crocidolite-treated lung cells, were also detected in

this study (Nymark et al. 2007). However, some of the magnitudes of gene expression alteration by chrysotile were not great, probably due to different molecular responses of BEAS-2B cells to different kinds of asbestos as reported in EGF receptor activation (Faux et al. 2000). Reported mesothelioma-associated genes named TPD52L1 (tumor protein D52-like 1), BIRC5 (baculoviral IAP repeat-containing 5 (survivin)), CALU (calumenin) and TXN (thioredoxin) were detected in the chrysotile-exposed BEAS-2B cells in this study. Other asbestos-related genes named chemokines, growth-regulated oncogene-alpha (Gro-alpha, CXCL-1), interleukin-8 (IL-8) and activating transcription factor 3 (ATF3), were also detected (Belitskaya-Levy et al. 2007).

Those genes that were reported to be common in some epithelial and mesothelial cell lines after exposure to crocidolite were also detected in this study. Among them, NOTCH2 was about 2-fold down-regulated by 20  $\mu\text{g}/\text{cm}^2$  chrysotile in this examination. Thioredoxin (TXN) was reported to potentially contribute to common responses to crocidolite in three epithelial and mesothelial lung cell lines (Nymark et al. 2007). However, the magnitude of TXN alteration was not great in this study. Asbestos-induced cytotoxicity and genotoxicity have been proposed to be associated with enhanced oxidative stress via production of reactive oxygen species (Kakooei et al. 2007). The genes involved in redox potential, including peroxiredoxin-1 (PRDX1), were also up-regulated by 20  $\mu\text{g}/\text{cm}^2$  chrysotile.

The regulatory and sorting mechanisms involved in internalization of toxicants by endocytosis are still poorly understood. However, the Rab family of small GTP-binding proteins plays crucial roles in regulating the trafficking pathways, and the Rab family is known to be directly implicated in regulating endocytic recycling of cell surface receptors and junctional proteins, as well as controlling cytoskeletal rearrangement (Chen et al. 2010). The RAB36, RAS oncogene family and G-protein-coupled receptor 18 were notably up-regulated by both concentrations of chrysotile.

Oxysterol-binding protein 2, a membrane-bound protein encoded by OSBP2, contains a pleckstrin homology (PH) domain and an oxysterol-binding region. The proteins in different organisms indicate roles of the gene family in diverse cellular processes including control of lipid metabolism, regulation of vesicle transport, apoptosis and cell signaling events (Lehto and Olkkonen 2003). One member of this family in humans, HLM/OSBP2 protein, has recently been reported as a potential marker for solid tumor dissemination and worse prognosis in these cases (Henriques et al. 2003). Therefore, about 3.2-fold up-regulation of OSBP by chrysotile might be involved in the tumor

transformation following exposure to chrysotile, although its precise function in the lung cells is not defined yet.

Even more interesting was the observation that SMC3 (structural maintenance chromosome 3), which is a key component of the nuclear multimeric protein complex named cohesion, was up-regulated approximately 3-fold at 20  $\mu\text{g}/\text{cm}^2$  chrysotile. SMC3 was reported to be elevated in human carcinomas, and the up-regulation of SMC3 expression was also suggested to be sufficient or permissive to trigger cell transformation through ras-rho/GTPase and cAMP signaling pathway (Ghiselli and Liu 2005). The up-regulation result for OSP2 and SMC3 in the microarray was well consistent with that in real-time PCR.

In conclusion, the result provides chrysotile-specific gene expression patterns, and the biological and metabolic processes of the genes might be implicated in the chrysotile toxicity. Also this study identifies several targets for further investigation in relation to asbestos-related diseases. In this regard, this profiling could confer insights into understanding the mechanism by which chrysotile affects the lung, and the genes modulated by chrysotile could serve as potential biomarkers for the prediction and diagnosis of chrysotile toxicity.

### Acknowledgements

This project was supported by Korea Ministry of Environment as SoonChunHyang Environmental Health Center for asbestos related disease.

### References

- Al-Wadei HM, Schuller HM. 2006. Cyclic AMP-dependent cell type-specific modulation of mitogenic signaling by retinoids in normal and neoplastic lung cells. *Cancer Detect Prev* 30:403–411.
- Belitskaya-Levy I, Hajjou M, Su WC, Yie TA, Tchou-Wong KM, Tang MS, Goldberg JD, Rom WN. 2007. Gene profiling of normal human bronchial epithelial cells in response to asbestos and benzo(a)pyrene diol epoxide (BPDE). *J Environ Pathol Toxicol Oncol* 26:281–294.
- Chen L, Hu J, Yun Y, Wang T. 2010. Rab36 regulates the spatial distribution of late endosomes and lysosome through a similar mechanism to Rab34. *Mol Membr Biol* 27:24–31.
- Dopp E, Yadav S, Ansari FA, Bhattacharya K, von Recklinghausen U, Rauen U, Rödelsperger K, Shokouhi B, Geh S, Rahman Q. 2005. ROS-mediated genotoxicity of asbestos-cement in mammalian lung cells in vitro. *Part Fibre Toxicol* 2:9.
- El-Said WA, Yea CH, Kim H, Oh BK, Choi JW. 2009. Cell-based chip for the detection of anticancer effect on HeLa cells using cyclic voltammetry. *Biosens Bioelectron* 24:1259–1265.
- Faux SP, Houghton CE, Hubbard A, Patrick G. 2000. Increased expression of epidermal growth factor receptor in rat pleural mesothelial cells correlates with carcinogenicity of mineral fibres. *Carcinogenesis* 21:2275–2280.
- Frank AL. 1993. Global problems from exposure to asbestos. *Environ Health Perspect* 3:165–167.
- Fung H, Kow YW, Van Houten B, Mossman BT. 1997. Patterns of 8-hydroxydeoxyguanosine formation in DNA and indications of oxidative stress in rat and human pleural mesothelial cells after exposure to crocidolite asbestos. *Carcinogenesis* 18:825–832.
- Fusello AM, Mandik-Nayak L, Shih F, Lewis RE, Allen PM, Shaw AS. 2006. The MAPK scaffold kinase suppressor of Ras is involved in ERK activation by stress and proinflammatory cytokines and induction of arthritis. *J Immunol* 177:6152–6158.
- Ghiselli G, Liu CG. 2005. Global gene expression profiling of cells overexpressing SMC3. *Mol Cancer* 4:1–34.
- Henriques SN, Vasconcelos FM, Pimenta G, Pulcheri WA, Spector N, Da Costa Carvalho Mda G. 2003. HLM/OSBP2 is expressed in chronic myeloid leukemia. *Int J Mol Med* 12:663–666.
- Kakooei H, Sameti M, Kakooei AA. 2007. Asbestos exposure during routine brake lining manufacture. *Ind Health* 45:787–792.
- Kim SJ, Park HW, Youn JP, HA JM, An YR, Lee CH, Oh MJ, Oh JH, Yoon SJ, Hwang SY. 2009. Genomic alteration of bisphenol A treatment in the testis of mice. *Mol Cell Toxicol* 5:216–221.
- Kortenjann M, Shaw PE. 1995. The growing family of MAP kinases: regulation and specificity. *Crit Rev Oncog* 6:99–115.
- Lehto M, Olkkonen VM. 2003. The OSBP-related protein: a novel protein family involved in vesicle transport, cellular lipid metabolism, and cell signaling. *Biochim Biophys Acta* 1631:1–11.
- Levchenko A, Bruck J, Sternberg PW. 2000. Scaffold proteins may biophysically affect the levels of mitogen-activated protein kinase signaling and reduce its threshold properties. *Proc Natl Acad Sci USA* 97:5818–5823.
- Li YL, Cheng XD, Hu Y, Zhou CY, Lü WG, Xie X. 2010. Identification of glia maturation factor beta as an independent prognostic predictor for serous ovarian cancer. *Eur J Cancer* 46:2104–2118.
- Loomis D, Dement J, Richardson D, Wolf S. 2010. Asbestos fibre dimensions and lung cancer mortality among workers exposed to chrysotile. *Occup Environ Med* 67:580–584.
- Malakhova OA, Yan M, Malakhov MP, Yuan Y, Ritchie KJ, Kim KI, Peterson LF, Shuai K, Zhang DE. 2003. Protein ISGylation modulates the JAK-STAT signaling pathway. *Genes Dev* 17:455–460.
- Ng DC, Bogoyevitch MA. 2000. The mechanism of heat shock activation of ERK mitogen-activated protein kinases in the interleukin 3-dependent ProB cell line BaF3. *J Biol Chem* 275:40856–40866.
- Nymark P, Wikman H, Ruosaari S, Hollmén J, Vanhala E, Karjalainen A, Anttila S, Knuutila S. 2006. Identification of specific gene copy number changes in asbestos-related lung cancer. *Cancer Res* 66:5737–5743.
- Nymark P, Lindholm PM, Korpela MV, Lahti L, Ruosaari S, Kaski S, Hollmén J, Anttila S, Kinnula VL, Knuutila S. 2007. Gene expression profiles in asbestos-exposed epithelial and mesothelial lung cell lines. *BMC Genomics* 8:62.
- Park EK, Hannaford-Turner KM, Hyland RA, Johnson AR, Yates DH. 2008. Asbestos-related occupational lung

- diseases in NSW, Australia and potential exposure of the general population. *Ind Health* 46:535–540.
- Rimbault M, Robin S, Vaysse A, Galibert F. 2009. RNA profiles of rat olfactory epithelia: individual and age related variations. *BMC Genomics* 10:572.
- Riml S, Schmidt S, Ausserlechner MJ, Geley S, Kofler R. 2004. Glucocorticoid receptor heterozygosity combined with lack of receptor auto-induction causes glucocorticoid resistance in Jurkat acute lymphoblastic leukemia cells. *Cell Death Differ Suppl* 1:S65–S72.
- Robin S, Tacher S, Rimbault M, Vaysse A, Dréano S, André C, Hitte C, Galibert F. 2009. Genetic diversity of canine olfactory receptors. *BMC Genomics* 10:21.
- Rossana B, Carlo C, Paola M, Giovanna Z. 2009. Rocks with asbestos: risk evaluation by means of an abrasion test. *Am J Environ Sci* 5:500–506.
- Shapiro P. 2002. Ras-MAP kinase signaling pathways and control of cell proliferation: relevance to cancer therapy. *Crit Rev Clin Lab Sci* 39:285–330.
- Shaul YD, Seger R. 2007. The MEK/ERK cascade: from signaling specificity to diverse functions. *Biochim Biophys Acta* 1773:1213–1226.
- Shukla A, Ramos-Nino M, Mossman B. 2003. Cell signaling and transcription factor activation by asbestos in lung injury and disease. *Int J Biochem Cell Biol* 35:1198–1209.
- Xu A, Wu LJ, Santella RM, Hei TK. 1999. Role of oxyradicals in mutagenicity and DNA damage induced by crocidolite asbestos in mammalian cells. *Cancer Res* 59:5922–5926.